Available online at www.sciencedirect.com
SCIENCE DIRECT®
International Journal of Heat and Mass Transfer 47 (2004) 4713–4720
International Journal of HEAT and MASS TRANSFER
www.elsevier.com/locate/ijhmt

Reverse flow regions in three-dimensional backward-facing step flow

J.H. Nie, B.F. Armaly *

Department of Mechanical and Aerospace Engineering, and Engineering Mechanics, University of Missouri—Rolla, Rolla, MO 65401, USA

Received 12 January 2004; received in revised form 27 May 2004
Available online 21 July 2004

Abstract

Laser-Doppler velocity measurements adjacent to the bounding walls of three-dimensional (3-D) backward-facing step flow are performed for the purpose of mapping the boundaries of the reverse flow regions that develop in this geometry (adjacent to the sidewalls, the flat wall and the stepped wall) as a function of the Reynolds number. The backward-facing step geometry is configured by a step height (S) of 1 cm, which is mounted in a rectangular duct having an aspect ratio (AR) of 8:1 and an expansion ratio (ER) of 2.02:1. Results are presented for a Reynolds number range between 100 and 8000, thus covering the laminar, transitional and turbulent flow regimes. The boundaries of the reverse flow regions are identified by locating the streamwise coordinates on a plane adjacent to the bounding walls where the mean streamwise velocity component is zero. The size of the reverse flow regions increases and moves further downstream in the laminar flow regime; decreases and moves upstream in the transitional flow regime; and remains almost constant or diminishes in the turbulent flow regime; as the Reynolds number increases. The spanwise distribution of the boundary line for the reverse flow region adjacent to the stepped wall develops a minimum near the sidewall in the laminar flow regime, but that minimum in the distribution disappears in the turbulent flow regime. Predictions agree well with measurements in the laminar flow regime and reasonably well in the turbulent flow regime.

1. Introduction

Separated-reattached flows due to sudden changes in geometry develop in many industrial devices such as fluidics, electronic and turbine blade cooling, and many other heat exchanging equipment. Thermal and momentum transports in the reattaching flow region and inside the reverse flow regions vary greatly, and that influences significantly the performance of these devices. For example, the minimum wall shear stress and the maximum heat transfer rate occur in the neighborhood of reattaching flow region on the stepped wall, while the minimum heat transfer rate occurs at the corner where the sudden change in geometry starts. Most of these industrial applications exhibit three-dimensional (3-D) behavior but most of the published studies are restricted to the two-dimensional (2-D) case. The size of the reverse flow region characterizes the global features of flow and heat transfer in this geometry, and it has been used in benchmark studies for validating two-dimensional

* Corresponding author. Tel.: +1 573 341 4601; fax: +1 573 341 4607.
E-mail address: armaly@umr.edu (B.F. Armaly).

0017-9310/$ - see front matter © 2004 Elsevier Ltd. All rights reserved.
doi:10.1016/j.ijheatmasstransfer.2004.05.027

Nomenclature

A	cross-sectional area of the upstream duct = $W\times h$	S	step height (= 1 cm)
AR	aspect ratio = W/S	u	mean velocity component in the x-direction
ER	expansion ratio = $H/(H-S)$	u_0	average inlet velocity
D_h	hydraulic diameter of the upstream duct = $4A/P$	v	mean velocity component in the y-direction
H	duct height downstream from the step (= 1.98 cm)	W	width of the duct (= 8 cm)
h	duct height upstream of the step (= 0.98 cm)	w	mean velocity component in the z-direction
L	half width of the duct (= $W/2$ = 4 cm)	x	coordinate in the streamwise direction
n	normal direction to the wall	x_u	location where the streamwise shear stress component is zero ($-\mu\frac{\partial u}{\partial n}\|_{\text{wall}}=0$)
P	wetted perimeter of the upstream duct = $2(W+h)$	y	coordinate in the transverse direction
Q	volumetric flowrate	z	coordinate in the spanwise direction
Re	Reynolds number = $\rho u_0 D_h/\mu$	*Greek symbols*	
		μ	dynamic viscosity
		ρ	density

simulation algorithms and codes (see, for example, [1–3]). Simulations and measurements of flow adjacent to the 2-D backward-facing step geometry have appeared extensively in the literature (see, for example, [4–7], and the references cited therein), but limited results have been published on the 3-D flow adjacent to this geometry.

Simulations of 3-D separated-reattached flow adjacent to backward-facing step by Chiang and Sheu [8,9], by Iwai et al. [10], and by Carrington and Pepper [11] revealed some of the complex laminar flow behaviors that develop in this geometry. Armaly et al. [12] illustrated the developments of a downwash adjacent to the sidewall, followed with swirling spanwise flow inside the primary reverse flow region, and a swirling "jet-like" flow that impinges on the stepped wall near the sidewall in this geometry. The strong spanwise flow that develops adjacent to the stepped wall makes it difficult to identify the reattachment region of this separated-reattached 3-D flow, as noted by Nie and Armaly [13,14]. Very few measurements of either local velocity or heat transfer have been published for this 3-D separated-reattached flow. Lim et al. [15], Shih and Ho [16], and Papadopoulos and Otugen [17] have published few measurements, and Armaly et al. [18] have presented measured distributions of the two velocity components for 3-D laminar backward-facing step flow. To the best of the authors' knowledge, the sizes and the distributions of the reverse flow regions that develop in this 3-D geometry adjacent to the bounding walls have not been measured or predicted for Reynolds numbers covering both the laminar and turbulent flow regimes. This fact, along with the realization that such a geometry appears regularly in many industrial heat transfer devices, motivated the present study.

2. Experimental apparatus and techniques

A schematic diagram of the experimental geometry is shown in Fig. 1. It consists of a backward-facing step in a duct where the step height is 1.0 cm (S) and the width is 8.0 cm (W). The coordinate system is defined as shown schematically in this figure, where the x-, y-, and z-coordinate directions denote the streamwise, the transverse, and the spanwise directions, respectively. The upstream section from the step is 0.98 cm in height (h) and 8.0 cm in width (W). The downstream section from the step is 1.98 cm in height (H) and 8.0 cm in width (W). This backward-facing step geometry is configured in the test section of the air tunnel that is shown schematically in Fig. 2. The open-air tunnel is constructed from Plexiglas sheets of 0.95 cm thick that are machined and assembled to form the desired geometry. The two sidewalls of the test section are made of 0.6 cm thick optical glass, thus facilitating the use of the laser-Doppler velocimeter (LDV) to measure, non-intru-

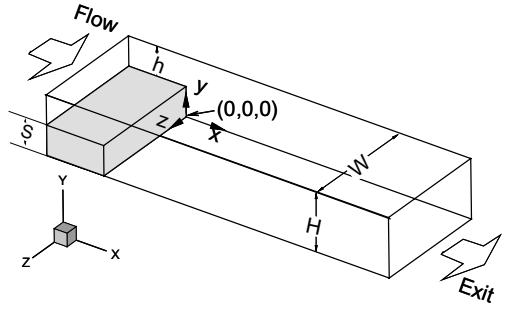

Fig. 1. Schematic of the backward-facing step geometry.

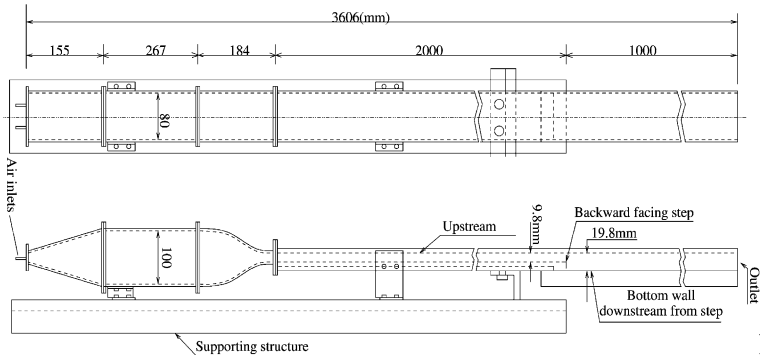

Fig. 2. Schematic of the air tunnel and test section.

sively, the local velocities. The upstream section of the air tunnel has the same cross-sectional area as the upstream section of the experimental geometry (0.98 cm in height and 8.0 cm in width), and it is 200.0 cm long. This length is sufficient to ensure fully developed airflow at the step. The downstream section of the air tunnel has the same cross-sectional area as the downstream section of the experimental geometry (1.98 cm in height and 8.0 cm in width), and it is 100.0 cm long. This length is sufficient to ensure fully developed flow at the exit section of the air tunnel. This geometry provides a backward-facing step with an expansion ratio (ER = H/h) of 2.02:1 and an aspect ratio (AR = W/S) of 8:1.

Air is supplied to the tunnel and the test section from a large high-pressure tank. The air passes through pressure regulation system that maintains a constant flow rate, at a selected level, with less than 1% variation. The air flow passes through a set of calibrated flow meters to determine the flow rate and the Reynolds number (Re). A fraction of the inlet airflow is bypassed through six jet atomizers and that air stream is seeded with olive oil particles having an average diameter of less than 0.6 μm. The seeded fraction of the airflow is mixed with the unseeded fraction in a large chamber at the inlet of the tunnel, and that mixture forms the seeded air stream that is supplied to the air tunnel. The inlet section of the tunnel consists of a diverging section, a straight section, and a converging section, as shown schematically in Fig. 2. The diverging section is packed with steel wool to remove any large oil particles from the seeded air, and the straight section is packed with honeycomb material for straightening the flow. The converging section has an area ratio of 10:1, and its smaller section connects directly to the upstream section of the tunnel, which is 200.0 cm long upstream of the step. This configuration ensures the development of fully developed airflow at the inlet of the backward-facing step. An aluminum frame is utilized to support the air tunnel in its vertical orientation.

A fiber optics laser-Doppler velocimeter was used to measure the streamwise velocity component (u) adjacent to the bounding walls that are downstream from the backward-facing step geometry. These measurements were used to identify the boundaries of the reverse flow regions that develop adjacent to the bounding walls, i.e. the streamwise locations where the mean streamwise velocity component (u) is zero on a plane adjacent to these walls (x_u-lines). The LDV system operated in a back-scattering mode and the focal length of the transmitting optics was 250 mm. The developing Doppler bursts were processed using Fourier transform analyzers and appropriate software. The measuring probe volume could be moved to any desired location, with an accuracy of less than 0.01 cm, in the flow field by a three-dimensional traverse mechanism. The traverse mechanism and the processing of the Doppler bursts were controlled by a personal computer. Repeated measurements established that 256–3000 acceptable LDV samples are sufficient to accurately determine the local mean streamwise velocity component in the flow domain. This number was dependent on the state of the flow (laminar or turbulent) and the measuring location in the flow field.

To ensure a steady state and stable flow conditions upstream of the step, the mean streamwise velocity component (u) was monitored and its distributions in the transverse and spanwise directions were measured upstream of the step at the center of the streamwise plane of $x/S = -1$. After ensuring that these inlet flow measurements are repeatable, measurements were initiated downstream from the step. The experimental repeatability was determined from measurements that were made at three different locations inside the air tunnel for a flow with a maximum inlet streamwise u-velocity of 4.25 m/s. The magnitudes of the velocities at the three different locations inside the test section were different, ranging from low near the walls to high at the center of the duct. The average velocity was measured repeatedly 12 times over a relatively short period of time, and 3000 valid Doppler signals were used to calculate the average velocity for

each of the 12 runs at each of the three locations. The deviation of any average velocity from the average of the 12 averaged values at any of the three locations was under ±0.025 m/s, and that establishes the uncertainty in these measurements.

3. Results and discussions

Measurements of the mean streamwise velocity components (u) adjacent to the bounding walls (i.e. the stepped wall ($y/S=0.05$), the side walls ($z/L=0.01$), and the flat wall ($y/S=1.95$)) downstream from the step are performed for the purpose of locating the boundaries of the reverse flow regions for different Reynolds numbers. These measurements were used to identify the mean streamwise locations (x) on these planes where the magnitude of the mean streamwise velocity component (u) is zero (or changing signs from positive to negative). These streamwise locations are identified and connected by a line, and these lines will be referred to as x_u-lines in the remaining part of this paper. The x_u-lines are approximately the boundaries of the reverse flow regions for the three-dimensional separated-reattached flow in this geometry as noted by Nie and Armaly [14]. The procedure for identifying this location (x_u-lines) in 2-D and 3-D flow in this geometry was described in an earlier study by Armaly et al. [5,18].

The following steps were followed in performing the LDV measurements. The LDV optics and the traverse system are aligned with the tunnel geometry to ensure that the traverse system is traversing in planes parallel to the test section in both the streamwise and the spanwise directions. The airflow rate through the tunnel is adjusted by the pressure regulator, and the volume flow rate (Q) is measured by the calibrated flow meter. The seeding density of the flowing air is adjusted by controlling the fraction of the airflow that is bypassed through the atomizers and by selecting the number of atomizers that are used for seeding the flow. The average inlet flow velocity is determined from its definition as $u_0=Q/A$, where A is the cross-sectional area of the upstream duct, and the Reynolds number is calculated using its definition as $Re=\rho u_0 D_h/\mu$. Different Reynolds numbers of flow can be obtained by readjusting the airflow rate through the tunnel. For each flow rate (Reynolds number), the distributions of the mean streamwise velocity component (u) are measured in the transverse direction at $z/L=1$ and the spanwise direction at $y/S=1.49$ in the upstream section of the step at $x/S=-1$. Measurements show that both the transverse velocity component (v) and the spanwise velocity component (w) in the upstream of the step are small enough to be negligible.

Measured transverse distributions of the mean streamwise velocity component in the upstream section of the step at $x/S=-1$ and $z/L=1$ are presented in Fig. 3 for different Reynolds numbers. The measured results are presented in dimensionless form (u/u_{max}) in order to examine the change in velocity distributions as a function of the Reynolds numbers. The maximum value of the mean streamwise velocity component (u_{max}) is at the center point of that plane, i.e. at $x/S=-1$, $y/S=1.49$ and $z/L=1.0$. The solid line in the figure is the velocity distribution that is proposed by Shah and London [19] for the fully developed laminar flow in the rectangular duct, and the measurements agree favorably with that distribution for Reynolds number smaller than 2555. Measured velocity distributions for Reynolds number smaller than 1703 (in the laminar regime for the upstream section of the step) are not presented in this figure, to maintain clarity in the figure, and they agree favorably with the fully developed laminar flow distribution (the solid line in the figure). The velocity distribution at the upstream section of step ($x/S=-1$) starts to deviate from the laminar fully developed flow distribution as the Reynolds number increases, indicating a transition from the laminar to the turbulent flow regime at that upstream section of the step. The distribution remains symmetric relative to the center of the duct, but becomes fuller as the Reynolds number continues to increase, as shown in this figure. The measured distributions almost stop varying for the Reynolds numbers equal to or higher than 4258, indicating a fully developed turbulent flow regime at the upstream section of the step ($x/S=-1$) for this and higher Reynolds numbers flow. The centerline (maximum) streamwise velocity component (u_{max}) at the upstream section of the step ($x/S=-1$, $y/S=1.49$ and $z/L=1$) is presented in Fig. 4 for different Reynolds numbers, and shows clearly the transition flow region from the laminar to the turbulent

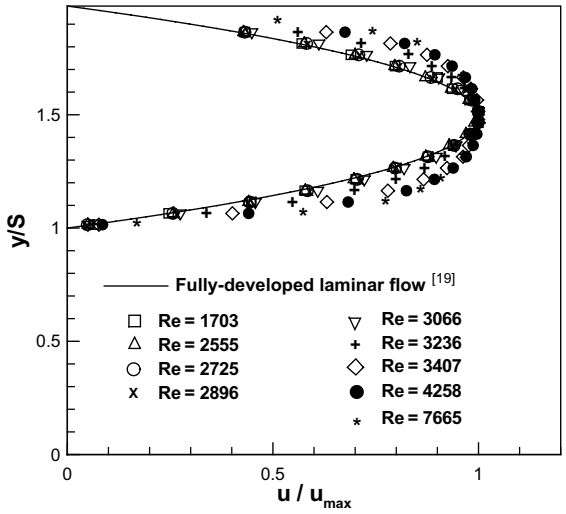

Fig. 3. Transverse distribution of the mean streamwise velocity component at $x/S=-1$ and $z/L=1$.

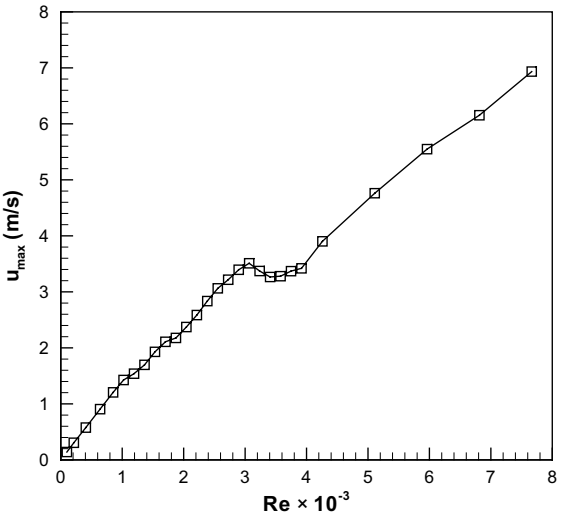

Fig. 4. Mean streamwise velocity component at the centerline of the inlet duct at $x/S=-1$ and $y/S=1.49$.

flow regime in the upstream section of the step. The centerline streamwise velocity component (u_{max}) at the upstream section of the step ($x/S=-1$, $y/S=1.49$ and $z/L=1$) in the transition flow regime ($Re=3300$–4500) remains approximately constant while the flow rate or the Reynolds number is increasing, and that is due to the changes that develop in the velocity distribution that is shown in Fig. 3 for this flow range. Otherwise, the measured centerline streamwise velocity component (u_{max}) in this upstream section of the step appears to be proportional to the flow rate, or Reynolds number, in both the fully laminar and the fully turbulent flow regimes.

Velocity measurements scans of the mean streamwise velocity component (u) are made on planes adjacent to the bounding walls downstream from the step (i.e. the stepped wall, the sidewall and the flat wall) and the mean streamwise location where that velocity component is equal to zero is determined and these locations are used to identify the x_u-line distribution. The x_u-line that was measured at the center of the test section ($z/L=1$) downstream from the step on a plane that is adjacent to the stepped wall ($y/S=0.05$) is presented in Fig. 5 as function of the Reynolds number. One to ten minutes of measurements, depending on the state of the flow and the location in the flow field, was needed to establish one point on this line. The 2-D results (in a duct with an aspect ratio of 36:1) that were reported by Armaly et al. [5] for the same parameter are presented in the same figure for comparison. The 2-D and the 3-D results for these distributions exhibit similar trends as the Reynolds number increases: an increase in the laminar flow regime, a sudden and sharp decrease in the transition flow regime, and almost constant in the fully turbulent

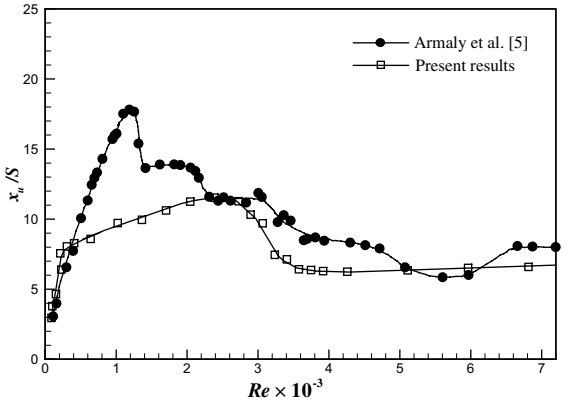

Fig. 5. Outer boundary of the reverse flow region at the center of the test section on a plane adjacent to the stepped wall (at $y/S=0.05$ and $z/L=1$).

flow regime ($Re>3400$). In comparison with the 2-D results: for the backward-facing step flow, the 3-D results are slightly higher in the laminar flow regime $Re<400$; significantly lower in the transition flow regime $400<Re<3400$; and slightly lower in the fully turbulent flow regime $Re>3400$. It should be noted that the starting and the ending values of the Reynolds numbers for the flow regimes in the upstream section of the step (the rectangular duct flow) are different than the flow regimes in the downstream section of the step (the backward-facing step flow).

Spanwise distributions of the x_u-line on a plane adjacent to the stepped wall ($y/S=0.05$) are presented in Fig. 6 for different Reynolds numbers. These lines are

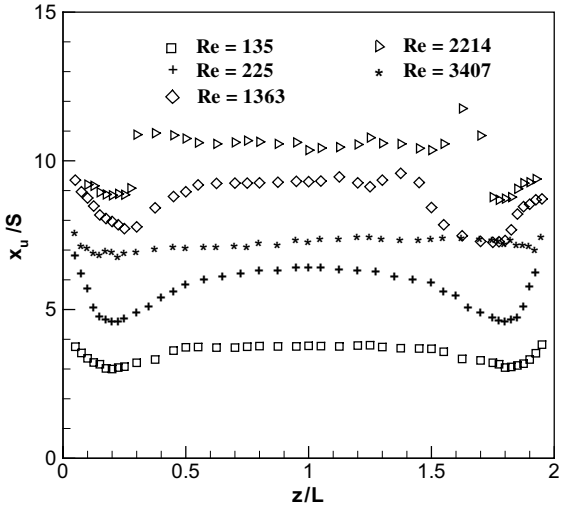

Fig. 6. Spanwise distributions of the x_u-lines on a plane adjacent to the stepped wall ($y/S=0.05$).

symmetric with respect to the center width of the duct ($z/L=1$) for low Reynolds number, i.e. $Re=135$ and 225, but lose some of this symmetry as the Reynolds number increases to the transition flow regime, i.e. $Re=1363$ and 2214. The x_u-line becomes symmetric again, however, in the fully turbulent flow regimes, i.e. $Re \geqslant 3406$. Fig. 6 also shows clearly how the x_u-line varies with increase of the Reynolds number: increases in the laminar flow regime, decreases rapidly in the transition flow regime, and remains approximately constant in the turbulent flow regime, as can also be seen in Fig. 5. These x_u-lines at the stepped wall ($y/S=0.05$) exhibit strong spanwise variations, with a minimum that develops at approximately $z/L=0.25$ and 1.75, and a maximum that develops at the sidewalls ($z/L=0$ and 2). The minimum in these distributions, which develops in the laminar flow regime, disappears in the fully turbulent flow regimes where the distribution is uniform in the center spanwise region for $0.2<z/L<1.8$ at $Re \geqslant 3406$. The complex flow behavior that develops in the laminar flow regime in this geometry is described in details by Armaly et al. [12] and Nie and Armaly [14]. The "jet-like" flow and the swirling flow that develop in the separating shear layer adjacent to the sidewall, impinge on the stepped wall causing the maximum and the minimum that appear in the spanwise distributions of the x_u-lines. The impingement region of the "jet-like" flow on the stepped wall is equivalent to the region where the x_u-line is a minimum near the sidewall. The rebounding fluid from the impingement region of the "jet-like" flow is responsible for the maximum that develops in the spanwise distribution of the x_u-lines at the sidewall, as noted by Nie and Armaly [14].

Measured streamwise distributions of the x_u-lines on a plane adjacent to the sidewall ($z/L=0.05$) and on a plane adjacent to the flat wall ($y/S=1.95$) of this geometry are presented in Figs. 7 and 8, respectively. The laminar flow results ($Re=135$ and 225) that are presented in these figures are generated using the flow simulation code that is described by Nie and Armaly [14]. The region enclosed by the x_u-lines adjacent to the sidewall represents approximately the size of the reverse flow region adjacent to the sidewall. The results presented in

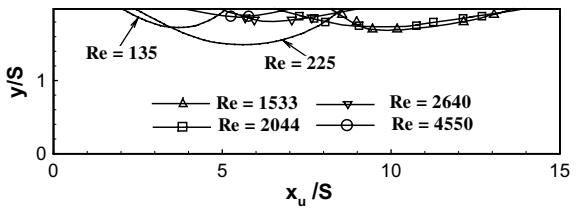

Fig. 7. Streamwise distributions of the x_u-lines on a plane adjacent to the sidewall ($z/L=0.05$).

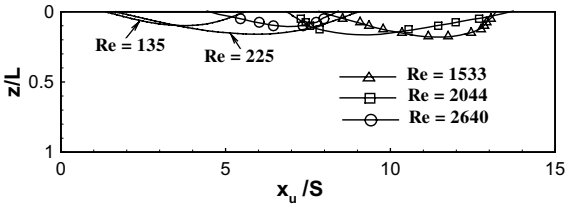

Fig. 8. Streamwise distributions of the x_u-lines on a plane adjacent to the flat wall ($y/S=1.95$).

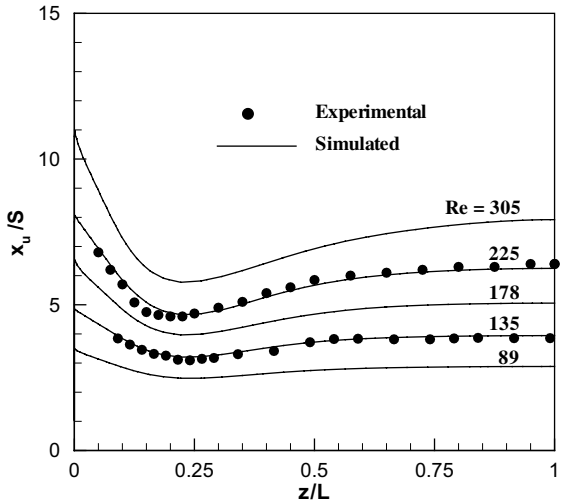

Fig. 9. Comparison between measured and simulated x_u-lines at $y/S=0.05$ (laminar flow).

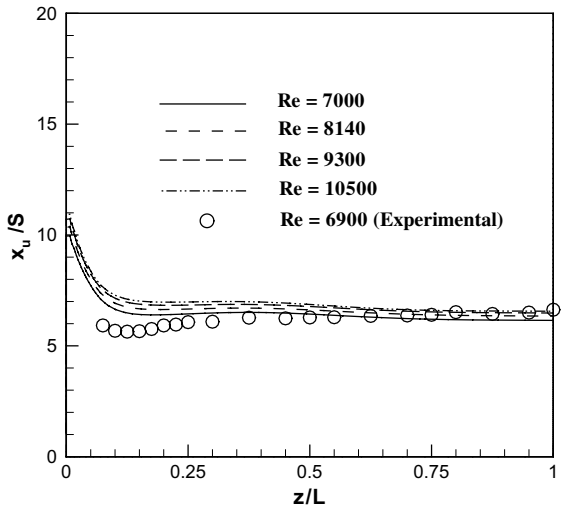

Fig. 10. Comparison between measured and simulated x_u-lines at $y/S=0.05$ (turbulent flow).

these figures indicate that the reverse flow regions bounded by these lines increase in size and moves further downstream as the Reynolds number increases in the laminar flow regimes, decreases and moves upstream in the transition flow regime, and decreases or diminishes in the turbulent flow regimes. Some comparisons between the simulated by Nie and Armaly [20] and the measured x_u-lines on a plane adjacent to the stepped wall ($y/S=0.05$) are presented for both laminar and turbulent flows in Figs. 9 and 10, respectively. The behavior of these boundary lines as a function of the Reynolds numbers can be seen more clearly in these figures. Measurements compare very favorably with simulations in the laminar flow regime and reasonably well in the turbulent flow regime.

4. Conclusions

Measurements of the boundaries of the reverse flow regions that develop adjacent to the bounding walls of a 3-D backward-facing step flow are presented as a function of the Reynolds number. The size of the reverse flow regions adjacent to the bounding walls, as described by the x_u-lines, is presented for the laminar, the transitional, and the turbulent flow regimes. In comparison with the reattachment point at the stepped wall for 2-D flow: the 3-D flow results at the center of the test section are slightly higher in the laminar flow regime ($Re<400$); significantly lower in the transition flow regime ($400<Re<3400$); and slightly lower in the fully turbulent flow regime as ($Re>3400$). The x_u-lines at the stepped wall exhibit strong spanwise variations in the laminar flow regime, with a minimum that develops at approximately $z/L=0.25$ and 1.75 near the sidewalls and a maximum that develops at the sidewalls ($z/L=0$ and 2), but the minimum in these distributions disappears in the turbulent flow regimes where the distribution becomes uniform in the center width region for $0.2<z/L<1.8$ for $Re \geqslant 3400$. The size of the reverse flow region adjacent to the sidewall and the flat wall in this geometry increases and moves further downstream in the laminar flow regime; decreases and moves upstream in the transition flow regime; and remains constant or diminishes in the turbulent flow regime; as the Reynolds number increases. Predictions agree well with measurements in the laminar flow regime and reasonably well in the turbulent flow regime.

Acknowledgment

This work was supported by a US Department of Energy Grant no. DE-FG02-03ER46067.

References

[1] B.F. Blackwell, D.W. Pepper (Eds.), Benchmark Problems for Heat Transfer Codes, HTD-vol. 222, American Society of Mechanical Engineers, New York, NY, 1992.
[2] B.F. Blackwell, B.F. Armaly (Eds.), Computational Aspects of Heat Transfer—Benchmark Problems, HTD-vol. 258, American Society of Mechanical Engineers, New York, NY, 1993.
[3] J.L. Sohn, Evaluation of FIDAP on some classical laminar and turbulent benchmarks, Int. J. Numer. Meth. Fluids 8 (12) (1988) 1469–1490.
[4] R.L. Simpson, Aspects of turbulent boundary-layer separation, Progress Aerosp. Sci. 32 (5) (1996) 457–521.
[5] B.F. Armaly, F. Durst, J.C.F. Pereira, B. Schonung, Experimental and theoretical investigation of backward-facing step flow, J. Fluid Mech. 127 (1983) 473–496.
[6] J.K. Eaton, J.P. Johnson, A review of research on subsonic turbulent flow reattachment, AIAA J. 19 (9) (1981) 1093–1100.
[7] S. Jovic, D.M. Driver, Backward-facing step measurements at low Reynolds number, $Re_h=5000$, NASA Technical Memorandum 108807, National Aeronautics and Space Administration, 1994.
[8] T.P. Chiang, T.W.H. Sheu, Vortical flow over a 3-D backward-facing step, Numer. Heat Transfer Part A—Appl. 31 (2) (1997) 167–192.
[9] T.P. Chiang, T.W.H. Sheu, A numerical revisit of backward-facing step flow problem, Phys. Fluids 11 (4) (1999) 862–874.
[10] H. Iwai, K. Nakabe, K. Suzuki, Flow and heat transfer characteristics of backward-facing step laminar flow in a rectangular duct, Int. J. Heat Mass Transfer 43 (3) (2000) 457–471.
[11] D.B. Carrington, D.W. Pepper, Convective heat transfer downstream of a 3-D backward-facing step, Numer. Heat Transfer Part A—Appl. 41 (6–7) (2002) 555–578.
[12] B.F. Armaly, A. Li, J.H. Nie, Three-dimensional forced convection flow adjacent to backward-facing step, AIAA J. Thermophys. Heat Transfer 16 (2) (2002) 222–227.
[13] J.H. Nie, B.F. Armaly, Three-dimensional convective flow adjacent to backward-facing step—effects of step height, Int. J. Heat Mass Transfer 45 (12) (2002) 2431–2438.
[14] J.H. Nie, B.F. Armaly, Reattachment of three-dimensional flow adjacent to backward-facing step, ASME J. Heat Transfer 125 (3) (2003) 422–428.
[15] K.S. Lim, S.O. Park, H.S. Shim, A low aspect ratio backward-facing step flow, Exp. Thermal Fluid Sci. 3 (5) (1990) 508–514.
[16] C. Shih, C.M. Ho, Three-dimensional recirculation flow in a backward facing step, ASME J. Fluids Eng. 116 (2) (1994) 228–232.
[17] G. Papadopoulos, M.V. Otugen, Separating and reattaching flow structure in a suddenly expanding rectangular duct, ASME J. Fluids Eng. 117 (1) (1995) 17–23.
[18] B.F. Armaly, A. Li, J.H. Nie, Measurements in three-dimensional laminar separated flow, Int. J. Heat Mass Transfer 46 (19) (2003) 3573–3582.
[19] R.K. Shah, A.L. London, Laminar Flow Forced Convection in Ducts, Academic, New York, 1978 pp. 196–198.

[20] J.H. Nie, B.F. Armaly, Three-dimensional turbulent forced convection flow adjacent to backward-facing step, in: K. Hanjalic, Y. Nagano, M.J. Tummers (Eds.), Proceedings of 4th International Symposium on Turbulence, Heat and Mass Transfer, Begell House, Antalya, Turkey, October 12–17, 2003.